Intra and extracellular surface charges near Ca^{2+} channels in neurons and neuroblastoma cells

Andrea Becchetti, Annarosa Arcangeli,* Maria Riccarda Del Bene,* Massimo Olivotto,* and Enzo Wanke
Department of General Physiology and Biochemistry, University of Milan, I-20133 Milano; and
*Institute of General Pathology, University of Florence, I-50134 Firenze, Italy

ABSTRACT The properties of low (LVA) and high (HVA) voltage-activated calcium currents were investigated in rat sensory neurons and a murine neuroblastoma cell line exposed to various concentrations of intra- or extracellular monovalent ($[c^+]_{i/o}$) and trivalent ($[c^{3+}]_{i/o}$) cations. In neurons, when $[c^+]_i$ was changed from 150 to 20 mM, positive shifts of 18–28 mV were observed in activation curves of both LVA and HVA currents, as well as in LVA inactivation curves. Extracellularly, in divalent-free solutions, $[c^+]_o$ of 20–50 mM produced medium (12–22 mV) negative shifts of the LVA channel properties. These data were used to estimate, by a "screening" model, a negative surface charge density around neuron's calcium channels of 1/1,000 and 1/1,325 $e\text{Å}^{-2}$ at the outside or inside face, respectively. In the presence of physiological concentrations of divalent cations, $[c^+]_o$ of 20–60 mM caused smaller (4–11 mV) negative shifts of the activation and inactivation curves, which can be explained by assuming a partial neutralization of negative charges by divalent cations. By applying the above procedure to LVA channels of neuroblastoma cells, the ratio of extra- to intracellular surface charge density turned out to be more than tenfold higher than in neurons. Effects produced by $[c^{3+}]_{i/o}$ were not in agreement with expectations based on screening or binding models.

INTRODUCTION

Gouy (1910) and Chapman (1913) proposed the first quantitative theory to describe the electrostatic behavior of a charged planar surface bathed by an electrolyte solution. This theory is simplified in many respects, principally because it assumes the existence of a uniformly smeared density (σ) of fixed charges and disregards possible cations binding to specific membrane sites. This "simple screening" model has been used to interpret the modifications of ion-channel voltage-dependent parameters, in the presence of solutions with different ionic composition (Chandler et al., 1965), leading to estimate the surface charge in the vicinity of various ion channels. Indeed, results obtained by lowering the extracellular concentration of monovalent cations around voltage-gated Na^+ channels were explained with reasonable accuracy by the screening model (Hille et al., 1975). On the other hand, supplementary assumptions were introduced to explain effects found after modification of divalent cation concentration or pH (e.g., Gilbert and Ehrenstein, 1969; Hille et al., 1975; Nonner et al., 1980; Wanke et al., 1979; Iijima et al., 1986).

Excellent reviews (McLaughlin, 1977, 1989), summarizing theory and recent results, also bring under the reader's attention several implications of electrostatic surface potentials in cellular physiology. It was shown that as different phenomena as exocytosis in sea urchin eggs (McLaughlin and Whitaker, 1988), interactions of PIP_2 with membrane proteins (Anderson and Marchesi, 1985) and interaction of protein kinase C with intracellular side of the plasma membrane (Mosior and McLaughlin, 1991) depend on peculiar properties of charged membranes.

Address correspondence to Dr. Wanke at the Department of General Physiology and Biochemistry, University of Milan, via Celoria 26, I-20133 Milano.

On the other hand, the surface potential of the external face of the plasma membrane is apparently implicated in the modulation of cell adhesion processes either with other cells or with extracellular matrices (Springer, 1990). To give some examples, the content of highly charged polysialic acid is an important regulator of NCAM-mediated adhesion (Rutishauser et al., 1988), whereas modifications on the extracellular membrane surface charge density leading to alteration of cell–cell adhesion mechanisms are considered to contribute to the development of metastatic phenotype in malignant cells. Furthermore, surface charges on phospholipids or on channel proteins themselves can influence in various ways ion permeation (for a review see Green and Andersen, 1991; Perozo and Bezanilla, 1990; Vandenberg and Bezanilla, 1991*a*, *b*).

In view of their steep voltage dependence and of their engagement in manifold cytosolic functions, calcium channels represent suitable targets of studies aimed at exploring the role of surface charge density in cell biology. However, very few data exist on extracellular surface potential around calcium channels (Ohmori and Yoshi, 1977; Kostyuk et al., 1982; Wilson et al., 1983; Cota and Stefani, 1984), none of which is on mammalian tissues, while no estimate exists of charge density around the intracellular portion of these channels.

We present here a study on the surface potential sensed by voltage-activated calcium channels (for a review see Carbone and Swandulla, 1989; Hess, 1991) on rat sensory neurons, based on measurements of whole cell currents before and after changing extra- or intracellular monovalent cation concentration ($[c^+]_o$, $[c^+]_i$) or trivalent cation concentration.

This study was extended to a murine neuroblastoma cell line (N1 cells) bearing LVA Ca^{2+} channels, to com-

0006-3495/92/10/954/12 $2.00

TABLE 1 **Values (in mV) of parameters k and $V_{1/2}$ of the Boltzmann curves shown in Figs. 4, 6, 7, and 8**

Fig.	IN/ OUT	$[c^{2+}]$	$[c^{+}]$	Activation k	Activation $V_{1/2}$	Shift measured	Shift corrected	Inactivation k	Inactivation $V_{1/2}$	Shift measured	Shift corrected
For DRG cells:											
4	OUT	4	150	−4.8	−36.0 ± 0.9			4.6	−47.3 ± 1.0		
	OUT	4	70	−5.1	−43.9 ± 0.8	−7.9	−4.3	4.3	−55.5 ± 1.1	−8.2	−4.8
	OUT	4	30	−5.4	−47.8 ± 1.1	−11.8	−4.0	6.0	−66.8 ± 1.4	−19.5	−11.7
6	OUT	0	150	−3.5	−6.92 ± 1.5			5.2	−94.3 ± 1.5		
	OUT	0	60	−2.9	−89.0 ± 1.3	−19.8	−15.8	4.8	−110.6 ± 2.4	−16.3	−12.3
	OUT	0	25	−2.1	−96.9 ± 1.8	−27.7	−19.7				
7	IN	0	150	−4.5	−36.0 ± 0.9			4.7	−41.0 ± 1.5*		
	IN	0	26	−3.7	−17.5 ± 1.1	17.5	17.5				
	IN	0	20	−3.4	−8.8 ± 0.5	26.2	26.2	4.0	−18.0 ± 1.0*	23.2	23.2
8	OUT	4	150	−5.1	−6.4 ± 0.4						
	OUT	4	70	−4.3	−14.7 ± 0.8	−8.3	−4.6				
	OUT	4	30	−3.3	−21.3 ± 0.5	−14.9	−7.1				
8	IN	0	150	−4.4	−11.2 ± 0.4						
	IN	0	50	−3.3	−7.2 ± 0.3	4.0	4.0				
	IN	0	40	−3.7	2.9 ± 0.5	14.1	14.1				
	IN	0	26	−3.4	6.3 ± 0.6	17.5	17.5				
	IN	0	20	−3.3	13.2 ± 0.8	24.4	24.4				
For N1 cells:											
6	OUT	0	150	−4.5	−72.2 ± 1.9			4.8	−102.0 ± 2.3		
	OUT	0	60	−4.0	−94.9 ± 2.1	−22.7	−19.2	5.5	−122.9 ± 2.1	−20.9	−17.4
	OUT	0	25	−4.8	−118.2 ± 2.9	−46.0	−39.0	4.7	−147.5 ± 1.9	−45.5	−38.5
7	IN	0	150	−4.0	−31.0 ± 1.3			4.6	−39.0 ± 0.6		

In the table are also indicated the shifts and the corrected values reported in Results and Figs. 1 and 2. The asterisk indicates that the experiment was performed with a preconditioning time of 0.2 s.

pare the results of our approach to the available studies, attributing a higher surface charge to malignant as compared to normal cells (Adam and Adam, 1975; Elul et al., 1975; Brown et al., 1979; Pretlow and Pretlow, 1979; Price et al., 1987; Gascoyne and Becker, 1990).

METHODS

Preparation of cells

DRGs were dissected from 1–2 day- old Sprague-Dawley rats and dissociated with collagenase and trypsin (Sigma Chemical Co., St. Louis, MO) [0.1%, 1:1]) incubating for 1 h at 37°C. The resulting suspension was plated onto 35 mm collagen coated dishes at a density of six spinal cord chains per dish. The plating medium was Ham's nutrient mixture F12 supplemented with 10% heat inactivated fetal calf serum (FCS), penicillin 1 U/ml, streptomycin 1 μg/ml, gentalyn 2 μg/ml, NGF (7S, Calbiochem) 0.5 μg/ml. Neurons (30–50-μm diameter) were used for 2 d after dissection.

N1 neuroblastoma cells (a subclone of 41A3 murine neuroblastoma), kindly provided by Professor G. Mugnai, Institute of General Pathology, University of Florence, were routinely cultured in Dulbecco's modified Eagle medium (DMEM) supplemented with glucose 24 mM and 10% FCS, and incubated at 37°C in a humidified atmosphere, with 10% CO_2 in air. Cells from a subconfluent culture were detached with 0.25% trypsin, centrifuged at 250 g for 10 min and resuspended in DMEM containing 250 μg/ml of BSA at a cell concentration of $3–5 * 10^4$ cells/ml. Usually 2 ml of this cell suspension were transferred in 35 mm petri dishes previously coated with BSA. Cells having diameters of 15–25 μm were used for patch-clamp experiments.

Solutions

For experiments in the presence of extracellular divalent cations

Extracellular solution for experiments with neurons contained (mM): 125 Tetraethylammonium chloride (TEACl), 2 KCl, 2 $CaCl_2$, 20 4-Aminopyridine, 1 $MgCl_2$, 10 HEPES, pH 7.3.

For N1 cells, in which the only inward current was the LVA Ca^{2+} current, the extracellular solution contained: 140 NaCl, 1 $MgCl_2$, 10 $CaCl_2$, 2 KCl and 10 HEPES. When needed, TEACl or NaCl were always substituted with sucrose, keeping the osmolarity constant.

Intracellular solution contained (mM): 100 Cs-aspartate, 20 TEA-Cl, 2 1,2-bis(2-Aminophenoxy)ethane N,N,N',N'-Tetraacetic acid (BAPTA), 5 Mg_2ATP, 10 HEPES (pH 7.4).

The voltage-dependent curves in different intracellular ionic conditions were obtained by using pipettes filled with different solutions on different neurons. DRG neurons (but not N1 cells) suffered particularly in the presence of low $[c^{+}]_i$ and only cells whose currents did not run down more than 25% in 5 min were considered reliable for analysis.

For experiments in the absence of extracellular divalent cations

During these measurements, calcium channels were made selective to monovalent ions (Kostyuk et al., 1983). This procedure also had the advantage of prolonging neurons' lifetimes during the experiments.

Extracellular (mM): 100 TEACl, 25 CsCl, 10 HEPES (pH 7.3); the calcium contaminations in salts and water were lowered by the addition of 100 μM BAPTA.

Intracellular (mM): 125 N-methyl-D-glucamine, 17 TEACl, 9 CsCl, 10 HEPES, 2 BAPTA.

Cs^{+} was preferred to Na^{+} because it was threefold less able to perme-

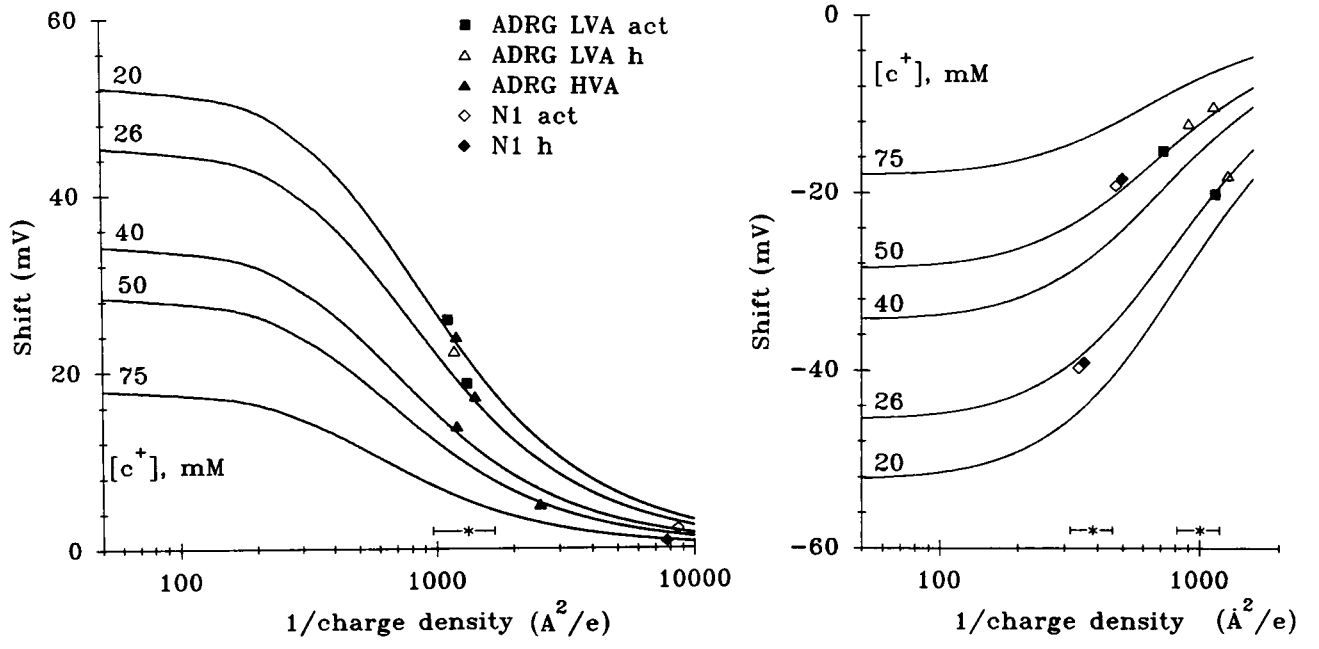

FIGURE 1 Shifts of Ca^{2+} channels voltage-dependent activation or inactivation (gating) versus the reciprocal of the charge density σ ($eÅ^{-2}$) produced by lowering $[c^+]_{i/o}$ with respect to physiological solutions. Curves correspond to the indicated values in mM and were derived from the Gouy-Chapman equation (see Theory). Symbols represent experimental shifts reported from Table 1. ADRG = sensory neurons, N1 = neuroblastoma cells, act = activation and h = inactivation. Asterisk indicates the mean of the experimental data. (*Left*) Intracellular (n = 19 for ADRG, n = 5 for N1). (*Right*) extracellular (divalent-free) (n = 3 for ADRG, n = 4 for N1).

ate in calcium channels (Lux et al., 1990). The extracellular Cs^+ concentrations used (25 mM) produced currents whose relatively small amplitude did not cause space-clamp artifacts. Furthermore, a small $[Cs^+]_i$ settled the Cs^+ inversion potential at ~ +15/25 mV. During these experiments, the solutions with low $[c^+]_o$ were obtained upon substitution of TEACl with sucrose, always maintaining both the osmolarity and $[Cs^+]_o$ constant. About 3–4 min of perfusion with the new solutions were necessary to produce a stationary level of Cs^+ currents. Preliminary experiments (not shown) demonstrated that a $[BAPTA]_o$ of 100 μM allowed us to measure LVA current; under this condition, the HVA currents became unmeasurable, in keeping with the report that a much higher $[BAPTA]_o$ is needed to unblock HVA channels (Lux et al., 1990), a finding attributed to a major affinity for calcium of the external binding sites of HVA as compared to LVA channels (Hess and Tsien, 1984; Almers and McCleskey, 1984). This high $[BAPTA]_o$ caused prohibitive leakage, especially at low ionic strength. For this reason, we decided to perform experiments in nominally divalent-free external solutions only on LVA channels.

Electrophysiological recordings

Whole-cell patch-clamp currents were recorded with the method of Hamill et al., 1981. Analog and digital (P/4 technique, Armstrong and Bezanilla, 1974) subtraction was used to correct all the current traces. Moreover, leakage and capacitive currents were subtracted from the control experiments as currents persisting in the presence of 100 μM of the Ca^{2+} channel blocker Cd^{2+} (with the same protocols, immediately after the control experiments); this blockade was always completely reversible. All experiments where recovery was less than 75%, after correcting for the run down, were disregarded. Our perfusing system was routinely checked to exclude possible contamination by Cd^{2+} ions, which are known to stick to walls of perfusing tubes. Liquid junction potentials V_j (used to correct the shifts reported in Results) were measured and found higher than a fraction of a mV only at low $[c^+]_o$ (range $[c^+]_o$ = 75/20 mM). Patch pipettes had resistances of 0.5–2 MΩ for sensory cells and 4–7 MΩ for cancer cells. To avoid space-clamp artifacts we always choose spherical neurons of moderate dimensions (20–30 μm) and applied pipette series resistance compensation (up to ~85%). The pClamp (Axon Instruments, Burlingame, CA) software and hardware were used during experiments and analysis.

Data analysis

The activation threshold and the voltage-dependence were used as criteria to distinguish LVA from HVA currents (Carbone and Swandulla, 1989; Fox et al., 1987; Wanke et al., 1989; Schroeder et al., 1990). Both LVA and HVA currents were usually measurable in sensory neurons while N1 neuroblastoma cells showed only LVA currents. In physiological solutions, activation thresholds were ≈ −45 and −20 mV for LVA and HVA channels, respectively, whereas the maximal currents were at ≈ −20 and +5. HVA currents were always elicited after completely inactivating LVA currents (see figure legends). When necessary, these HVA recordings were used to correct LVA currents at −20 mV for contamination by HVA currents.

The activation and the steady-state inactivation curves were obtained from the ratio of peak current amplitudes I normalized to maximal current I_{max} (Fox et al., 1987; Kass and Krafte, 1987). Actually, the voltage-dependent parameter is the current divided by the driving force (i.e., the conductance). However, in our experiments the current reversals were in the range +70/+80 mV or +15/+25 mV when measuring Ca^{2+} or Cs^+ currents, respectively. Thus, the membrane potentials around which we found the maximal currents were always far from reversal potentials, so that omission of the driving force term leaded to negligible imperfections. An estimate of the errors introduced by this type of analysis was evaluated on the data reported in Fig. 6. The current amplitudes for $[c^+]_o$ = 150 and 22 mM were divided by the corresponding driving forces and normalized values were plotted in this figure (*open circles*), showing a negligible difference as compared to uncorrected data. We did not use the more rigorous method of evaluating the fraction of open channels through the instantaneous tail currents (e.g., Vandenberg and Bezanilla, 1991) because this method was unsuitable for relatively short experiments as ours needed to be.

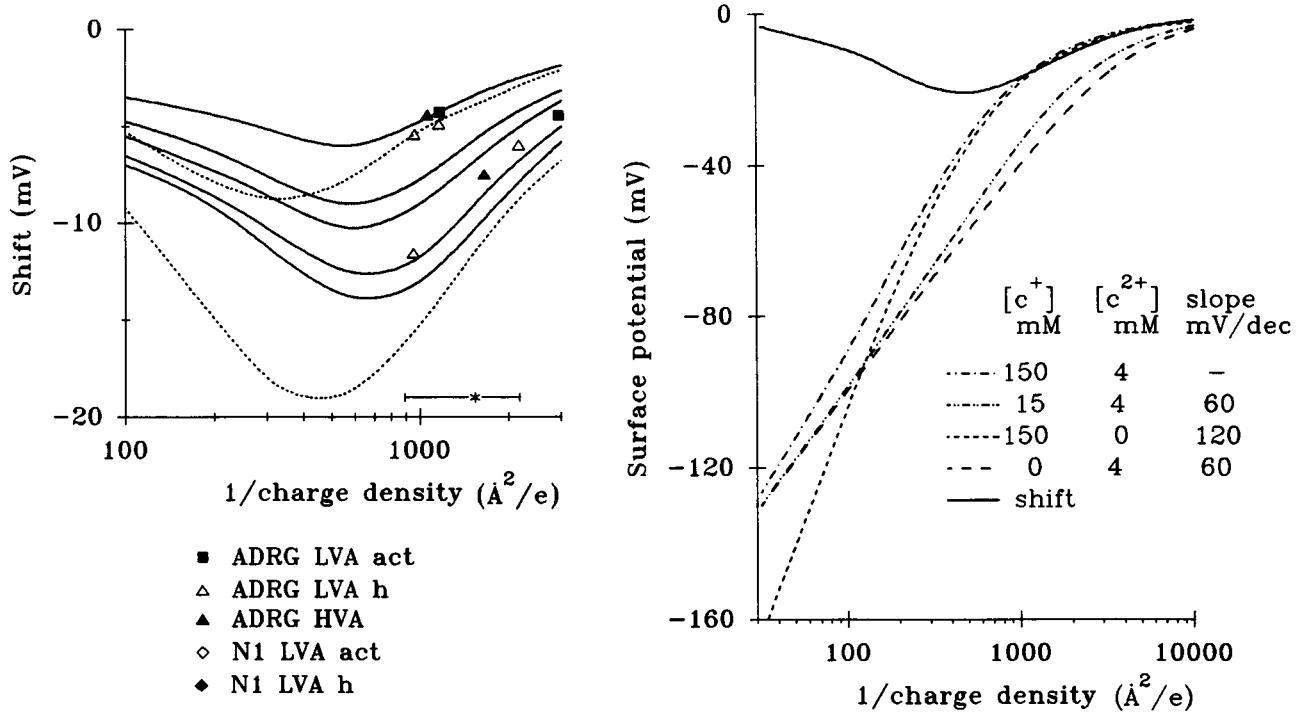

FIGURE 2 (*Left*) Shifts of the Ca^{2+} channel gating versus $1/\sigma$ produced by lowering $[c^+]_o$ with respect to physiological solutions (divalent ions present). Dotted lines represent solutions of the Grahame equation for bathing media containing $[c^+]_o$ = 75 and 20 mM and $[c^{2+}]_o$ = 4 mM. Continuous lines (for $[c^+]_o$ = 75, 50, 40, 26, and 20 mM, from the top to the bottom) were derived by assuming the supplementary condition that divalent cations neutralize a fraction of negative charges (see text). Symbols (whose meaning is the same as in Fig. 1) represent experimental shifts (n = 12). (*Right*) Surface potential versus $1/\sigma$ in the presence of the indicated different ion compositions as obtained from the Grahame equation. The continuous line represents the difference between the first two indicated curves, i.e., a voltage shift analogous to those shown on the left panel.

The ratios I/I_{max} were fitted with the Boltzmann relation

$$I/I_{max} = \{1 + \exp[(V_m - V_{1/2})/k]\}^{-1},$$

where the $V_{1/2}$ and k values are reported in Table 1.

As shown in Figs. 4, 5, and 8, we observed (but did not investigate) an increase of the peak currents at moderate $[c^+]_o$ (75–50 mM). These preliminary observations might suggest that higher negative electrostatic potentials increase the local carrier concentration (which is constant in the bulk solution), thereby producing higher currents (Iijima et al., 1986).

The surface potential Φ_o of the Grahame equation (see below) was derived from the roots of the polynomial associated to the equation itself after suitable calculation of the coefficients, which depend on the ionic composition of solutions (Asystant program, Macmillan Software Company, New York, NY). For all remaining analysis and the graphics, the Sigma Plot program (Jandel Sci., Corte Madera, CA) was used.

THEORY

The relation between the charge density σ and the surface potential Φ_o is satisfactorily described by the Gouy-Chapman theory, provided that the only effect of ions present in the bathing solution is charge screening. When using solutions containing various concentrations $[c_i]$ of ions of different valence z_i, the above relation is usually described by the Grahame equation (Abramson and Muller, 1933; Grahame, 1947):

$$\sigma^2 G^2 = \sum_i [c_i]\{\exp(-z_i e\Phi_o/kT) - 1\},$$

where k is the Boltzmann's constant, T is the absolute temperature, e is the elementary electron charge and G is a constant equal to 270 $(Å^2 e^{-1})(M^{1/2})$, at room temperature.

The Grahame equation can also be modified to take into account the divalent cation binding to discrete components of the surface under study (Gilbert et al., 1970; Hille et al., 1975). In this case σ is assumed to be

$$\sigma = \sigma_f/(1 + K[c^{2+}] \exp[-2e\Phi_o/kT]),$$

where σ_f is the density of the fixed titratable negative sites, K is the equilibrium constant of the binding reaction and $[c^{2+}]$ is the divalent cation concentration.

The shifts of Φ_o predicted by the Grahame equation for changes in intra and extracellular cations (mono and trivalent) are represented in Figs. 1–3 with the sign corresponding to the expected effect on activation or inactivation of hypothetical voltage-dependent channels located within the plasma membrane. These shifts are plotted versus the average area per elementary charge (the reciprocal of the charge density σ). In divalent-free solutions the shifts are monotonic functions of $1/\sigma$ (Fig. 1). On the contrary, in the presence of divalent cations the curves

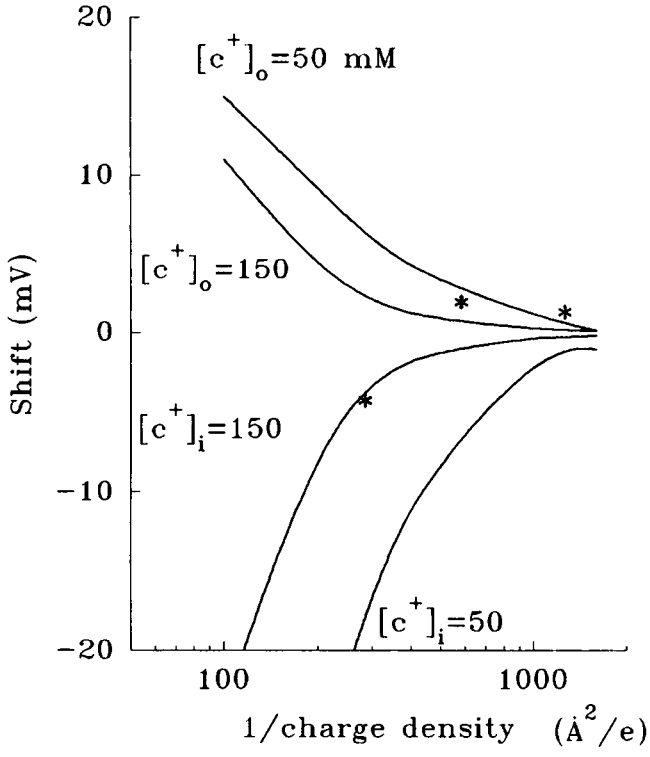

FIGURE 3 Shifts of the Ca^{2+} channels gating versus $1/\sigma$ produced by the intra (*lower*, $[Ca^{2+}]$ = 0 mM) or extracellular (*upper*, $[Ca^{2+}]$ = 4 mM) addition of 0.5 mM trivalent cations in the presence of various $[c^+]_o$. Curves were derived from the Grahame equation. Asterisks correspond to experimental shifts reported in Results (intracellular determinations n = 8; extracellular determinations for $[c^+]_o$ = 70, n = 4, for $[c^+]_o$ = 40, n = 3) (see text).

are no longer monotonic and the shifts' magnitude is about halved as compared to that predicted in the absence of divalent cations (Fig. 2, *left*). This is expected because GC theory predicts a stronger screening action of divalent cation. This effect is prevailing for highly charged membranes (small values of $1/\sigma$). Changes of monovalent ions concentrations (as we did) exert weak effects in the presence of divalent ions.

It is necessary to recall that these shifts derive from differences between the surface potentials $\Phi_o(1/\sigma)$ calculated in control conditions and at the particular value of $[c^+]$. To understand the reason for the counter intuitive appearance of the biphasic shape it is useful to observe the behavior of $\Phi_o(1/\sigma)$ in our conditions and in two limiting conditions of pure mono- and divalent salt solutions. In Fig. 2, *right*, $\Phi_o(1/\sigma)$ and the corresponding shift (*continuous line*) are shown in an instance very similar to ours (a tenfold change in monovalent cation concentration). The other two curves correspond to divalent- and monovalent-free cases: it is clear that, in the high charged region, the limiting slopes are 120 and 60 mV/decade, respectively. It appears also that the cases at $[c^{2+}]$ = 4 mM and $[c^+]$ = 15 mM (and $[c^{2+}]$ = 4) are almost coincident suggesting a prevailing action of divalent cations and a trivial action of monovalent cations (McLaughlin, 1977, p. 81).

In Fig. 2, *left*, the dotted lines represent the solutions of the Grahame equation for $[c^+]_o$ = 75 and 20 mM, in the presence of divalent cations (2 mM Ca^{2+} plus 2 mM Mg^{2+}). Notice that the magnitude of these shifts is about halved as compared to that predicted in the absence of divalent cations.

The full lines in Fig. 2, *left*, represent the solutions of the Grahame equation, for various $[c^+]_o$ from 75 to 20 mM, under the assumption that divalent cations neutralized charged sites of the membrane with an equilibrium constant K = 4 M^{-1} (see previous equation). This value was selected after a best fitting procedure to the experimental data and is not far from values previously reported for artificial bilayers and biological membranes (Hille et al., 1975; McLaughlin et al., 1981).

In Fig. 3, the effects of 0.5 mM of trivalent cations predicted by the Grahame equation are reported either for intracellular addition in the presence of $[c^+]_i$ = 150 and 50 mM, or for extracellular addition in the presence of $[c^+]_o$ = 150 and 50 mM, and $[c^{2+}]_o$ = 4 mM.

RESULTS AND DISCUSSION

Experimental data are necessarily reported without correction for V_j in Figs. 4–8. However, shifts need to be reported in Figs. 1–3 and in the following paragraph after correction. For easy reference we reported both experimental and corrected shifts also in Table 1.

Shifts of LVA channel activation and inactivation

Effects of changing $[c^+]_o$

In physiological external Ca^{2+} and Mg^{2+} solutions: upper panels of Fig. 4 show the typical LVA current traces evoked in neurons over the range −60 to −15 mV (holding = −90 mV) in the presence of various $[c^+]_o$. The somewhat unexpected lowering of peak currents at $[c^+]_o$ = 30 mM with respect to 70 mM is probably due to a partial inactivation caused by the holding potential used. Activation and steady-state inactivation data shown in Fig. 4 (*lower panels*) refer to six neurons treated with $[c^+]_o$ = 150 (control), 70 and 30 mM. Averaged shifts, calculated from the best fitting activation curves and corrected for V_j, resulted −4 ± 0.3 and −4.3 ± 0.4 mV for $[c^+]_o$ = 70 and 30 mM, respectively. By applying the same procedure for inactivation data, shifts were found −4.4 ± 0.2 and −11.7 ± 0.5 mV for $[c^+]_o$ = 70 and 30 mM, respectively. In some neurons, shorter preconditioning potential durations (0.2 s) were used and the calculated shifts were not significantly different (data not shown but pooled in Fig. 2). Substituting Ca^{2+} with Ba^{2+} (not shown) did not produce any significant difference.

In divalent-free external Cs^+ solutions: Fig. 5 shows experiments where LVA channels were made permeable to Cs^+ (see Methods) in neurons (*upper panels*) or

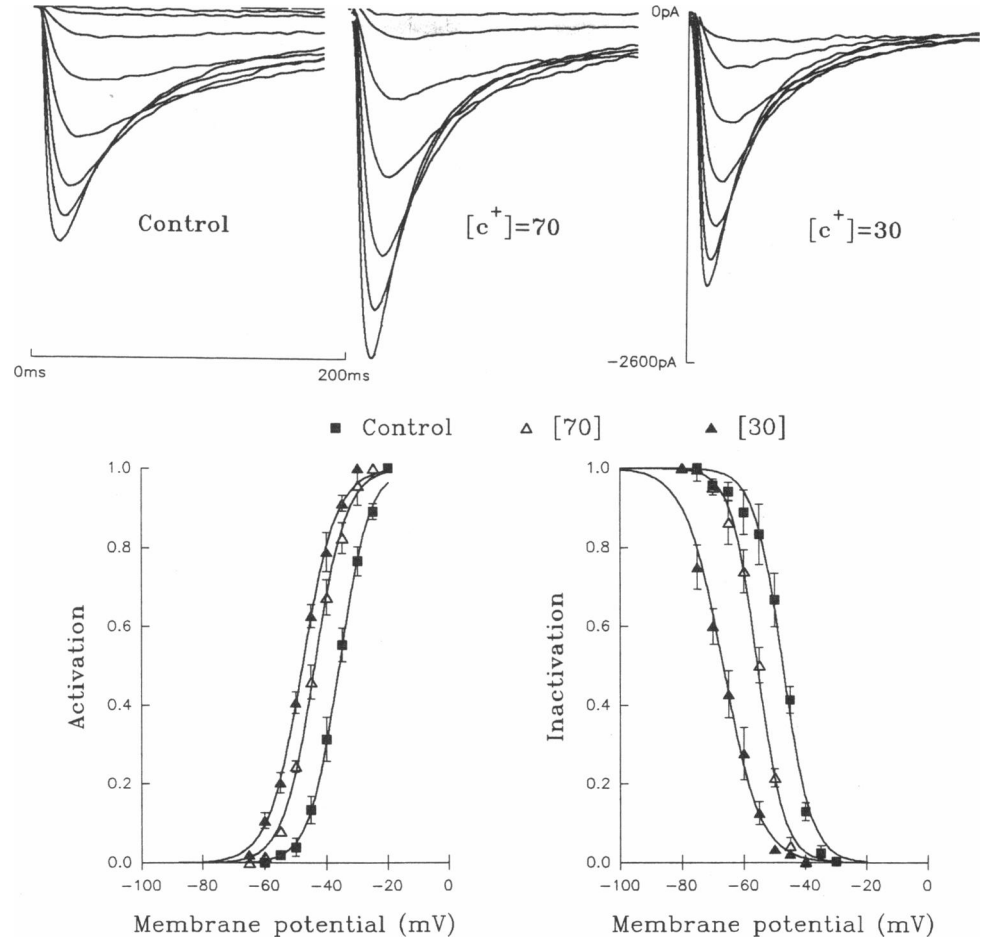

FIGURE 4 Effects of extracellularly applied low $[c^+]_o$ solutions with $[c^{2+}]_o$ = 4 mM, on LVA Ca^{2+} channels of sensory neurons. (*Upper panels*) Ca^{2+} currents traces at the indicated $[c^+]_o$. The holding potential (V_{hold}) and test potentials (V_{test}) were as follows; for controls, V_{hold} = −90, V_{test} = −50/−15 (step = 5 mV); for $[c^+]_o$ = 70 and 30 mM, V_{hold} = −90, V_t = −60/−30 (step = 5 mV). (*Lower panels*) Activation and inactivation curves. Symbols represent experimental data pooled from six neurons. The best fitting curves were obtained by the Boltzmann equation (see Table 1 and Methods). The process of inactivation was studied with a V_{test} = −20 mV and a preconditioning time of 1 s.

N1 cells (*lower panels*) with different $[c^+]_o$ and constant $[Cs^+]_o$.

Removal of divalent cations at $[c^+]_o$ = 150 mM (Fig. 6) produced activation curves whose $V_{1/2}$ values were about 33 mV and 42.2 mV more negative than corresponding values shown in Fig. 4, for DRG neurons and N1 cells, respectively (see also Table 1). These differences were much larger than those predicted on the basis of the Grahame equation indicating a substantial deviation from the Gouy-Chapman theory (see later).

From Fig. 6 it is possible to calculate that in neurons the shifts of the activation curves were −15.8 ± 0.85 and −19.6 ± 0.9 mV at $[c^+]_o$ = 60 and 25 mM, respectively, and the shift of the inactivation curves at $[c^+]_o$ = 60 mM was −12.3 ± 0.7 mV (*upper panels*). Other data (not shown) obtained with a shorter inactivation time gave shifts of −11.5 (at [60]mM) and −18.2 (at [25]mM) mV. The shifts in N1 cells were −19.2 ± 0.9 and −39.0 ± 1.3 mV (activation); −17.4 ± 1.1 and −38.5 ± 1.5 mV (inactivation) at $[c^+]_o$ = 60 and 25 mM (*lower panels*).

The time constants of activation (τ_m) and inactivation (τh) of LVA Cs^+ currents are reported in Table 2, for $[c^+]_o$ = 150 and 60 mM. It is evident that lowering $[c^+]_o$ causes a 3–4 fold decrease in τ_m at −50/−60 mV, and in τ_h at −80 mV.

Effects of changing $[c^+]_i$

The activation and inactivation curves for neuron calcium channels are shown in Fig. 7 (*upper*). The corrected shifts for activation were 17.5 ± 1.1 and 26.2 ± 1.3 mV at $[c^+]_i$ = 26 and 20 mM, while for inactivation the shift was 23 ± 2 mV at $[c^+]_i$ = 20 mM. Fig. 7 (*lower*) shows that no significant shift occurred in neuroblastoma cells at $[c^+]_i$ = 50 and 22 mM.

Shifts of HVA channel activation

Effects of changing $[c^+]_o$

Fig. 8 (*upper*) shows typical HVA current traces elicited from a holding potential of −35 mV, by step depolarization starting from −25 mV, at the indicated $[c^+]_o$ values.

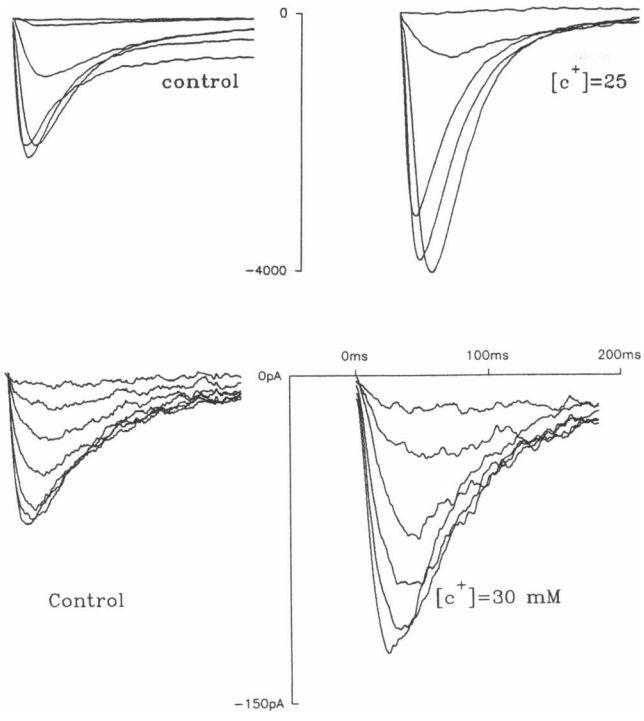

FIGURE 5 LVA Cs^+ current traces under the indicated low $[c^+]_o$ solutions. (*Upper panels*) rat sensory neuron. V_{hold} and V_{test} were as follows: for controls, $V_{hold} = -120$, $V_t = -90/-40$ (step = 10 mV); for $[c^+]_o$ = 25, $V_{hold} = -135$, $V_t = -110/-70$ (step = 10 mV). (*Lower panels*) N1 cell. V_{hold} and V_{test} were as follows: for controls, $V_{hold} = -120$, $V_t = -75/-45$ (step = 5 mV); for $[c^+]_o = 30$, $V_{hold} = -145$, $V_t = -115/-90$ (step = 5 mV).

The results of six activation experiments are summarized in Fig. 8 (*lower left*) leading to calculated shifts of -4.6 ± 0.3 and -7.1 ± 0.7 mV at $[c^+]_o = 70$ and 30 mM, respectively. Similar experiments ($n = 3$) were performed in the presence of 4 mM Ba^{2+} instead of 2 mM Ca^{2+} with negligible differences (not shown).

Effects of changing $[c^+]_i$

Data obtained under these conditions were pooled in the lower right panel of Fig. 8. The corrected shifts of the activation curves were 4 ± 0.3, 14.1 ± 0.6, 17.5 ± 0.8, and 24.4 ± 1.2 mV at $[c^+]_i$ = 50, 40, 26, and 20 mM, respectively.

The estimate of intracellular surface charge

Voltage shifts measured at various $[c^+]_i$ were reported on the corresponding ordinate values and curves in Fig. 1, obtaining estimates of the internal surface charge density. Symbols, referring to both activation and inactivation of either LVA or HVA neuron currents, fell in a narrow abscissa range leading to estimate an average charge density of $1/(1325 \pm 360)$ eÅ^{-2}.

In the case of N1 cells, experimental shifts fell within a range of the plot where curves converged so that one can only safely conclude that the charge density was lower than 1/9,500 eÅ^{-2}.

The estimate of extracellular surface charge

Experimental shifts referring to changes of $[c^+]_o$ in the absence of divalent cations are reported in Fig. 1 (*right*), giving the following estimates: $1/(1{,}000 \pm 200)$ eÅ^{-2} for neurons and $1/385 \pm 80$ eÅ^{-2} for N1 cells.

Based on these estimates, the Grahame equation gives, in control conditions, Φ_o equal to -18 and -50 mV for neurons and N1 cells, respectively. Assuming a binding of divalent cations (Fig. 2, *right*) the corresponding Φ_o values predicted become -16.5 and -38.5 mV. Thus, after addition of divalent cations, the maximal theoretically-expected shift values are -1.5 and -11.5 mV, while we found -33 and -42.2 mV. On the other hand, under similar experimental conditions, shift values which fitted well the theory were reported using the Na^+ channel in frog nerve (Hille et al., 1975) or muscle (Campbell and Hille, 1976; Hahin and Campbell, 1983) and in unmyelinated nerve (Vandenberg and Bezanilla, 1991*a*). Thus, for Ca^{2+} channels, other factors than cation adsorption should be invoked to account for this

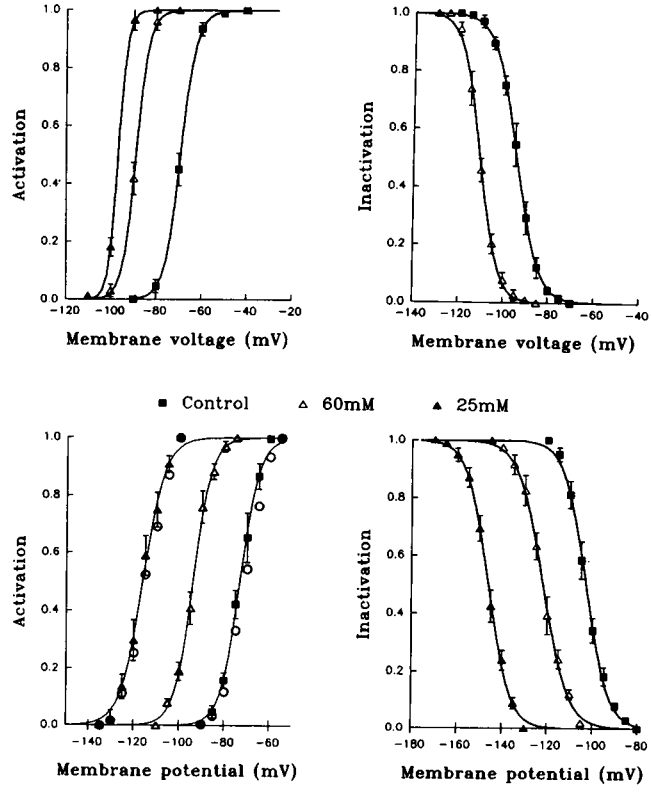

FIGURE 6 Effects of low $[c^+]_o$ solutions on LVA channels gating (Cs^+ as current carrier). The lines are Boltzmann curves which best fitted the experimental points (see Table 1 for values). For inactivation, V_{test} was always chosen as to obtain the maximal possible current, based on the results of activation data. (*Upper panels*) sensory neurons ($n = 3$); (*lower panels*) neuroblastoma cells ($n = 4$). Open circles in the left lower panel represent conductance data evaluated as explained in Methods (data analysis).

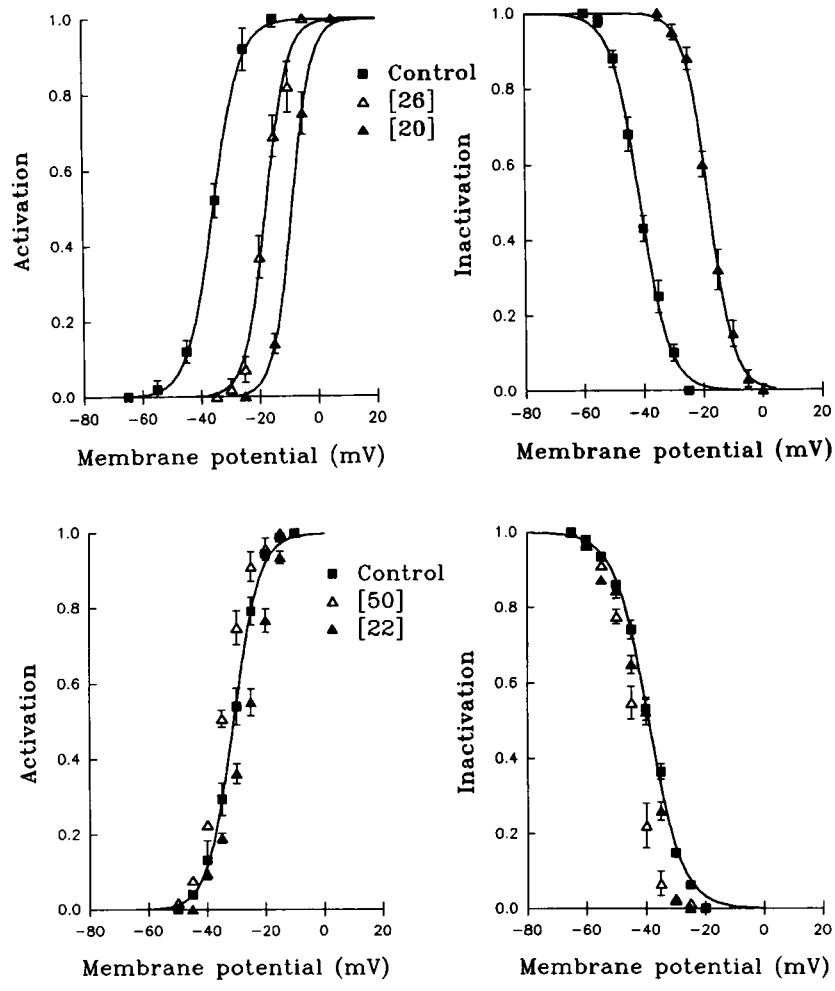

FIGURE 7 Effects of low $[c^+]_i$ solutions on LVA channels gating of sensory neurons (*upper panels;* activation, $n = 4$; inactivation, $n = 2$) and N1 cells (*lower panels,* $n = 5$). The lines are Boltzmann curves which best fitted the experimental points (see Table 1 for the values). Preconditioning time in the inactivation protocols was 0.2 s; V_{test} was chosen with the rationale explained in the legend of Fig. 6.

discrepancy, possibly some changes in the properties of the pore mouth charge distribution of the channel, as proposed for the Na^+ channel (Cai and Jordan, 1990).

In the presence of divalent cations and different $[c^+]_o$ (Fig. 2, *left*), data obtained for both activation and inactivation for either LVA and HVA channels in neurons were superimposed to the right limbs of the curves (*solid lines,* binding model), in view of the charge density estimate previously obtained in the absence of divalent cations. The average value resulted to be 1/1,535 ± 640 eÅ^{-2} not far from 1/(1,000 ± 200) eÅ^{-2}. On the other hand, a tentative insertion of the same experimental points on curves derived from a simple "screening" model (*dashed lines*) suggested a much higher average charge density, thus, indicating that the binding model is more appropriate.

Effects of trivalent cations on LVA and HVA activation

The effects of trivalent cations were tested both intracellularly (La^{3+}) or extracellularly (Fe^{3+}), either in neurons or in N1 cells. We used Fe^{3+} for extracellular additions because, at difference with La^{3+}, Fe^{3+} turned out to be ineffective on these channels.

Intracellular 0.5 mM La^{3+} produced a shift of −5.4 ± 0.7 mV (mean application time = 10 min; $n = 8$) in the activation of the HVA currents. These results are not in agreement with our estimates of σ_i (1/1,325 ± 360 eÅ^{-2}) which lead to predict no shift in the presence of trivalent cations (see Fig. 3).

Extracellular 0.5 mM Fe^{3+} produced no measurable effect on neuron HVA currents, at $[c^+]_o = 150$ mM, and only 2.1 ± 0.2 and 2.6 ± 0.2 mV when tested at $[c^+]_o = 70$ and 40 mM, respectively.

Activation curves of LVA currents in N1 cells were not affected by Fe^{3+}, even when applied at $[c^+]_o = 30$ mM in divalent free solutions ($n = 5$). On the contrary, the extracellular charge density previously estimated (1/375 ± 50 eÅ^{-2}) leads to predict shifts around 8–10 mV at $[c^+]_o = 30$ mM (Fig. 3).

These results are in keeping with previous indications that the effects of trivalent cations are largely unpredict-

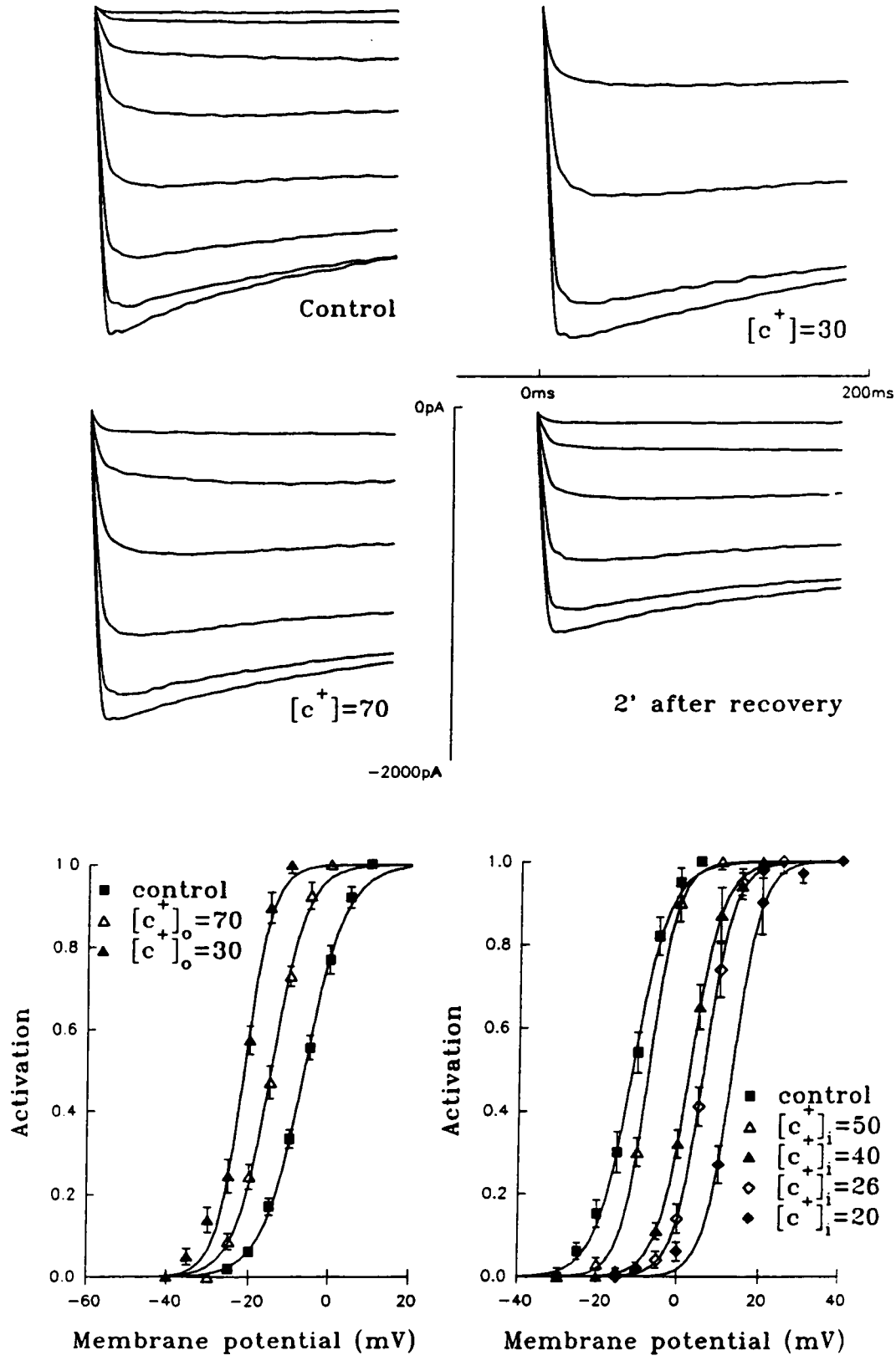

FIGURE 8 Effects of low $[c^+]_o$ and $[c^+]_i$ solutions on the HVA channels gating of sensory neurons. (*Upper panel*) Ca^{2+} currents before, during and after extracellular application of solutions containing the indicated $[c^+]_o$. V_{hold} = −35 mV; V_{test} beginning from −25 mV, steps of 5 mV. Solutions with low $[c^+]_o$ were maintained for at least 2 min (70 mM) or 3 min (30 mM). The large conductance increase observed at 30 mM was not further investigated. (*Lower panels*) lines are Boltzmann curves which best fitted the activation data for extra- (*left*, n = 6) and intra-cellular cation substitutions (*right*, $[c^+]_i$ = 50, n = 6; $[c^+]_i$ = 40, n = 5; $[c^+]_i$ = 26, n = 4; $[c^+]_i$ = 20, n = 4; see Table 1 for the values).

TABLE 2 **Time constants (ms) of LVA Cs^+ currents in rat sensory neurons, at various $[c^+]_o$ (see text, errors were derived from the fitting procedure)**

	$[c^+]_o$			
	150 mM	150 mM	60 mM	60 mM
Voltage (mV)	τ_m	τ_h	τ_m	τ_h
−100			14.2 ± 0.9	91 ± 2.5
−90			18.7 ± 1.1	38 ± 1.7
−80	9.1 ± .5	120 ± 4	10.2 ± .9	30 ± 1.3
−70	10.2 ± .7	64 ± 3	6.1 ± .4	28 ± 2
−60	8.5 ± .9	34 ±	3.1 ± .2	30 ± 2
−50	5.2 ± 1	29 ± 1.6	1.9 ± .2	30 ± 1.5
−40	3.3 ± .5	31 ± 2.3		

able on the basis of the Gouy-Chapman theory (Takata et al., 1966; Vogel, 1974; Arhem, 1980; Brismar, 1980; Neumcke and Stämpfli, 1984; Armstrong and Cota, 1990).

CLOSING REMARKS

The experimental approach used in this study turned out to be suitable to estimate the density charge around calcium channels on both sides of the plasma membrane. The main merit of this approach is that intra- and extracellular measurements were obtained for the same type of channel and by means of an unique technical procedure leading to an evaluation of the ratio of charge density on both membrane sides, that crucially affects the channel behavior.

Previous measurements of the charge density of the external surface (σ_e) provided a quite large range of values, with no apparent correlation of species, tissue or even channel type.

In fact, studies on potassium channels gave estimates varying from 1/64 to 1/600 $eÅ^{-2}$ in a broad spectrum of species (Mozhayeva and Naumov, 1970; Begenisich, 1975; Kell and DeFelice, 1988; Gilbert and Ehrenstein, 1969; Schauf, 1975; Carbone et al., 1978), while 1/70–1/588 $eÅ^{-2}$ is the reported range for Na^+ channels (Kostyuk et al., 1982; Brismar, 1973; Drouin and Neumcke, 1974; Vogel, 1974; Hille et al., 1975; Begenisich, 1975).

Experiments on calcium channels provided values around 1/250 $eÅ^{-2}$ in mammalian heart ventricles (Kass and Krafte, 1987), 1/500 $eÅ^{-2}$ in the frog muscle (Cota and Stefani, 1984), 1/434 $eÅ^{-2}$ in mollusc neurons (Kostyuk et al., 1982) and 1/80 $eÅ^{-2}$ in the tunicate oocyte and snail neuron membrane (Ohmori and Yoshii, 1977; Wilson et al., 1983).

The only studies we know concerning the internal surface charge (σ_i) were performed on the Na channel in the squid axon. By using an approach very similar to ours, Chandler et al. (1965) estimated σ_i = 1/740 $eÅ^{-2}$, while data derived under different experimental conditions offered values in the range 1/300–1/1,000 $eÅ^{-2}$ (Begenisich and Lynch, 1974; Wanke et al., 1979; Carbone et al., 1981; Perozo and Bezanilla, 1990).

One of the main points to emerge from our study is the substantial similarity between σ_e and σ_i in DRG neurons, both $\approx$1/1,000 $eÅ^{-2}$. This finding is rather surprising in view of the widely accepted tenet that the cytoplasmic face of the plasma membrane is less charged than the outer face (Hille, 1991). Although it seems difficult to attribute any biological meaning to this finding without knowing the screening power and binding properties of physiological media, the equivalence of σ_i and σ_e could suggest an equivalence of the surface electrostatic potential on both sides of the membrane.

In neuroblastoma cells σ_i resulted very low (<1/9,500 $eÅ^{-2}$) not only as compared to that measured in neurons but also as compared to σ_e (1/385) of the same cell. The latter value, although within the range reported for normal cells is three fold higher than in sensory neurons. It follows that in N1 cells the ratio $\sigma_e/\sigma_i \approx 25$, clearly far from that found for neurons.

Without the use of chemical reagents to specific charged groups it is not easy to discriminate between charges located on the channel protein and those on membrane portion surrounding the channel. For example, it is known that voltage-dependent channels possess extensive sugar domains of which a large fraction corresponds to sialic acid residues (Catterall, 1986). Their probable location on the external surface of the channel could influence the gating machinery and this is testable with aid of neuraminidase which specifically cleaves the sialic acid residues (Recio-Pinto et al., 1990).

Species difference as well as the long-term adaptation in culture of N1 cells, as compared to neurons, makes it difficult to attribute the surface charge peculiarity of neuroblastoma cells to the acquisition of the malignant phenotype. However this remarkable feature is certainly worth further exploration in a more appropriate model, such as neuroblastoma cells before and after differentiating treatments, or in sensory neurons immortalized and/or transformed by transfection with oncogenes.

The authors thank Dr. E. Carbone for kindly reading a preliminary version of this manuscript and Dr. G. Biella for preparing the sensory neurons.

This work was supported by grants from Ministero dell' Università e della Ricerca Scientifica e Tecnologica (MURST) (40%) to E. Wanke and Associazione Italiana per la Ricerca sul Cancro (AIRC) to M. Olivotto. A. Becchetti and M. Riccarda Del Bene were supported by AIRC fellowships. A. Arcangeli was supported by an Associazione Italiana per la Leucemia (AIL) fellowship.

Received for publication 18 February 1992 and in final form 15 June 1992.

REFERENCES

Abramson, H. A., and H. Muller. 1933. The influence of salts on the electric charge of surfaces in liquids. *Cold Spring Harbor Symp. Quant. Biol.* 1:29–33.

Adam, G., and G. Adam. 1975. Cell surface charge and regulation of cell division of 3T3 cells and transformed derivatives. *Exp. Cell Res.* 93:71–78.

Almers, W., and E. W. McCleskey. 1984. Non-selective conductance in calcium channels of frog muscle: calcium selectivity in a single file pore. *J. Physiol. (Lond.).* 353:585–608.

Anderson, R. A., and V. T. Marchesi. 1985. Regulation of the association of membrane skeletal protein 4.1 with glycophorin by a phosphoinositide. *Nature (Lond.).* 318:295–298.

Arhem, P. 1980. Effects of rubidium, caesium, strontium, barium and lanthanum on ionic current in myelinated nerve fibres from *Xenopus leavis*. *Acta Physiol. Scand.* 108:7–16.

Armstrong, C. M., and F. Bezanilla. 1974. Charge movement associated with the opening and closing of the activation gates of the Na channels. *J. Gen. Physiol.* 63:533–552.

Armstrong, C. M., and G. Cota. 1990. Modification of sodium channel gating by lanthanum. Some effects that cannot be explained by surface charge theory. *J. Gen. Physiol.* 96:1129–1140.

Begenisich, T. 1975. Magnitude and location of surface charges in *Mixicola* giant axon. *J. Gen. Physiol.* 66:47–65.

Begenisich, T., and C. Lynch. 1974. Effects of internal divalent cations on voltage-clamped squid axon. *J. Physiol. (Lond.).* 62:675–689.

Brismar, T. 1973. Effects of ionic concentration on permeability properties of nodal membran in myelinated nerve fibres of *Xenopus laevis*. Potential clamp experiments. *Acta Physiol. Scand.* 87:474–484.

Brismar, T. 1980. The effect of divalent and trivalent cations on the sodium permeability of myelinated nerve fibres of *Xenopus laevis*. *Acta Physiol. Scand.* 108:23–29.

Brown, A. E., K. R. Case, H. B. Bosmann, and A. C. Sartorelli. 1979. Cell surface charge alteration occurring during dimethylsulfoxide-induced erythrodifferentiation of Friend leukemia cells. *Biochem. Biophys. Res. Commun.* 86:1281–1287.

Cai, M., and P. C. Jordan. 1990. How does vestibule surface charge affect ion conduction and toxin binding in a sodium channel? *Biophys. J.* 57:883–891.

Campbell, D. T., and B. Hille. 1976. Kinetic and pharmacological properties of the sodium channel of frog skeletal muscle. *J. Gen. Physiol.* 67:309–323.

Catteral, W. A. 1986. Molecular properties of voltage-sensitive sodium channels. *Annu. Rev. Biochem.* 55:953–985.

Carbone, E., R. Fioravanti, G. Prestipino, and E. Wanke. 1978. Action of extracellular pH on Na^+ and K^+ membrane currents in the giant axon of *Loligo Vulgaris*. *J. Membr. Biol.* 43:295–315.

Carbone, E., and D. Swandulla. 1989. Neuronal calcium channels: kinetics, blockade and modulation. *Prog. Biophys. Mol. Biol.* 54:31–58.

Carbone, E., P. L. Testa, and E. Wanke. 1980. Intracellular pH and ionic channels in the Loligo vulgaris giant axon. *Biophys. J.* 35:393–413.

Chandler, W. K., A. L. Hodgkin, and H. Meves. 1965. The effect of changing the internal solution on sodium inactivation and related phenomena in giant axons. *J. Physiol. (Lond.).* 180:821–836.

Chapman, D. L. 1913. A contribution to the theory of electrocapillarity. *Phil. Mag.* 25:475–481.

Cota, G., and E. Stefani. 1984. Saturation of calcium channels and surface charge effects in skeletal muscle fibres of the frog. *J. Physiol.* 351:135–154.

Drouin, H., and B. Neumcke. 1974. Specific and unspecific changes at the sodium channels of the nerve membrane. *Pfluegers Arch. Eur. J. Physiol.* 351:207–229.

Elul, R., J. Brons, and K. Kravitz. 1975. Surface charge modifications associated with proliferation and differentiation in neuroblastoma cultures. *Nature (Lond.).* 258:616–617.

Fox, A. P., M. C. Nowycky, and R. W. Tsien. 1987. Kinetic and pharmacological properties distinguishing three types of calcium currents in chick sensory neurones. *J. Physiol. (Lond.).* 394:149–172.

Gascoyne, P. R. C., and F. F. Becker. 1990. Alterations in electrophoretic mobility, diaphorase activity, and terminal differentiation induced in murine erythroleukemia lines by differentiating agents. *J. Cell. Physiol.* 142:309–315.

Gilbert, D. L., and G. Ehrenstein. 1969. Effect of divalent cations on potassium conductance of squid axons: determination of surface charge. *Biophys. J.* 9:447–463.

Gilbert, D. L., and G. Ehrenstein. 1984. Membrane surface charges. *Curr. Top. Membr. Transp.* 22:407–421.

Gouy, G. 1910. Sur la constitution de la charge eletrique a la surface d'un electrolyte. *J. Physique.* 9:457–468.

Grahame, D. C. 1947. The electrical double layer and the theory of electrocapillarity. *Chem. Rev.* 41:441–501.

Green, W. N., and O. S. Andersen. 1991. Surface charges and ion channel function. *Annu. Rev. Physiol.* 53:341–359.

Hamill, O., A. Marty, E. Neher, B. Sakmann, and F. J. Sigworth. 1981. Improved patch-clamp techniques for high resolution current recording from cells and cell-free membrane patches. *Pfluegers Arch. Eur. J. Physiol.* 391:85–100.

Hahin, R., and D. T. Campbell. 1983. Simple shifts in the voltage dependence of sodium channel gating caused by divalent cations. *J. Gen. Physiol.* 82:785–805.

Hess, P. 1990. Calcium channels in vertebrate cells. *Annu. Rev. Neurosci.* 13:337–356.

Hess, P., and R. W. Tsien. 1984. Mechanism of ion permeation through calcium channels. *Nature (Lond.).* 308:453–456.

Hille, B. 1991. Ionic Channels in Excitable Membranes. Sinauer Associates Inc., Sunderland, MA.

Hille, B., M. Woodhull, and B. I. Shapiro. 1975. Negative surface charge near sodium channels of nerve: divalent ions, monovalent ions and pH. *Philos. Trans. R. Soc. Lond. B Biol. Sci.* 270:301–318.

Hodgkin, A. L., and A. F. Huxley. 1952. A quantitative description of membrane current and its application to conduction and excitation in nerve. *J. Physiol.* 117:500–544.

Iijima, T., S. Ciani, and S. Hagiwara. 1986. Effects of the external pH on Ca channels: experimental studies and theoretical considerations using a two-site, two-ion model. *Proc. Natl. Acad. Sci. USA* 83:654–658.

Kass, R. S., and D. S. Krafte. 1987. Negative surface charge density near heart calcium channels. Relevance to block by dihydropyridines. *J. Gen. Physiol.* 89:629–644.

Kell, M. J., and L. J. DeFelice. 1988. Surface charge near the cardiac inward-rectifier channel measured from single-channel conductance. *J. Membr. Biol.* 102:1–10.

Kostyuk, P. G., S. L. Mironov, P. A. Doroshenko, and V. N. Ponomarev. 1982. Surface charges on the outer side of mollusc neuron membrane. *J. Membr. Biol.* 70:171–179.

Kostyuk, P. G., S. L. Mironov, and Y. M. Shuba. 1983. Two ion-selecting filters in the calcium channel of the somatic membrane of mollusc neurons. *J. Membr. Biol.* 76:83–93.

Lux, H. D., E. Carbone, and H. Zucker. 1990. Na currents trough low-voltage activated Ca^{2+} channels of chick sensory neurons: block by external Ca^{2+} and Mg^{2+}. *J. Physiol.* 430:159–188.

McLaughlin, S. 1977. Electrostatic potentials at membrane-solution interfaces. *Curr. Top. Membr. Transp.* 9:71–143.

McLaughlin, S. 1989. The electrostatic properties of membranes. *Annu. Rev. Biophys. Biophys. Chem.* 18:113–36.

McLaughlin, S., N. Mulrine, T. Gresalfi, G. Vaio, and A. McLaughlin. 1981. Adsorption of divalent cations to bilayer membranes containing phosphatidilserine. *J. Gen. Physiol.* 77:445–473.

McLaughlin, S., G. Szabo, and G. Eisenman. 1971. Divalent ions and the surface potential of charged phospholipid membranes. *J. Gen. Physiol.* 58:667–687.

McLaughlin, S., and M. Whitaker. 1988. Cations that alter surface potentials of lipid bilayers increase the calcium requirement for exocytosis in sea urchin eggs. *J. Physiol.* 396:189–204.

Mosior, M., and S. McLaughlin. 1991. Peptides that mimic the pseudosubstrate region of protein kinase C bind to acidic lipids in membranes. *Biophys. J.* 60:149–159.

Mozhayeva, G. N., and A. P. Naumov. 1970. Effect of surface charge on the steady-state potassium conductance of nodal membrane. *Nature (Lond.).* 228:164–166.

Neumcke B., and R. Stämpfli. 1984. Heterogeneity of external surface charges near sodium channels in the nodal membrane of frog nerve. *Pfluegers Arch. Eur. J. Physiol.* 401:125–131.

Nonner, W., B. C. Spalding, and B. Hille. 1980. Low intracellular pH and chemical agents slow inactivation gating in sodium channels of muscle. *Nature (Lond.).* 284:360–363.

Ohmori, H., and M. Yoshii. 1977. Surface potential reflected in both gating and permeation of sodium and calcium channels of the tunicate egg cell membrane. *J. Physiol. (Lond.).* 267:429–463.

Perozo, E., and F. Bezanilla. 1990. Phosphorylation affects voltage gating of the delayed rectifier K^+ channel by electrostatic interactions. *Neuron.* 5:685–690.

Pretlow, T. G., and T. P. Pretlow. 1979. Cell electrophoresis. *Int. Rev. Cytol.* 61:85–127.

Price, J. A. R., R. Pethig, C. Lai, F. F. Becker, P. R. C. Gascoyne, and A. Szent-Gyôrgyi. 1987. Changes in cell surface charge and transmembrane potential accompanying neoplastic transformation of rat kidney cells. *Biochim. Biophys. Acta.* 898:129–136.

Recio-Pinto, E., W. B. Thornhill, D. S. Duch, S. R. Lewinson, and B. W. Urban. 1990. Neuraminidase treatment modifies the function of electroplax sodium channels in planar lipid bilayers. *Neuron.* 5:675–684.

Rutishauser, U., A. Acheson, A. K. Hall, D. M. Mann, and J. Sunshine. 1988. The neural cell adhesion molecule (NCAM) as a regulator of cell–cell interaction. *Science* (Wash. DC). 240:53–57.

Shauf, C. L. 1975. The interactions of calcium channels with Myxicola giant axons and a description in terms of a simple surface charge model. *J. Physiol. (Lond.).* 248:613–624.

Schroeder, J. E., P. S. Fishbach, and E. W. McCleskey. 1990. T-type calcium channels: heterogeneous expression in rat sensory neurons and selective modulation by phorbol esters. *J. Neurosci.* 10:947–951.

Springer, T. A. 1990. The sensation and regulation of interactions with the extracellular environment: the cell biology of limphocyte adhesion receptors. *Annu. Rev. Cell Biol.* 6:359–402.

Takata, M., W. F. Pickard, J. Y. Lettvin, and J. W. Moore. 1966. Ionic conductances changes in lobster axon membrane when lanthanum is substituted for calcium. *J. Gen. Physiol.* 50:461–471.

Vogel, W. 1974. Calcium and Lanthanum effect at the nodal membrane. *Pfluegers Arch. Eur. J. Physiol.* 350:25–39.

Vandenberg, C. A., and F. Bezanilla. 1991*a*. Single channel, macroscopic, and gating currents from sodium channels in the squid giant axon. *Biophys. J.* 60:1499–1510.

Vandenberg, C. A., and F. Bezanilla. 1991*b*. A sodium channel gating model based on single channel, macroscopic ionic, and gating currents in the squid giant axon. *Biophys. J.* 60:1511–1533.

Wanke, E., E. Carbone, and P. L. Testa. 1979. K^+ conductance modified by titratable group accessible to protons from the intracellular side of the squid axon embrane. *Biophys. J.* 26:319–324.

Wanke, E., A. Becchetti, L. Bertollini, and A. Ferroni. 1989. Cross-talk between receptors coupled to calcium currents in adult but not in neonatal rat sensory neurons. *Cell Biol. Int. Rep.* 13:1165–1175.

Wilson, D. L., K. Morimoto, Y. Tsuda, and A. M. Brown. 1983. Interaction between calcium ions and surface charge as it relates to calcium currents. *J. Membr. Biol.* 72:117–130.